Clinical Cancer Research

Identification of Rigosertib for the Treatment of Recessive Dystrophic Epidermolysis Bullosa–Associated Squamous Cell Carcinoma

Velina S. Atanasova[1], Celine Pourreyron[2], Mehdi Farshchian[1], Michael Lawler[1], Christian A. Brown IV[1], Stephen A. Watt[2], Sheila Wright[2], Michael Warkala[1], Christina Guttmann-Gruber[3], Josefina Piñón Hofbauer[3], Ignacia Fuentes[4,5], Marco Prisco[1], Elham Rashidghamat[6], Cristina Has[7], Julio C. Salas-Alanis[8], Francis Palisson[4,9], Alain Hovnanian[10,11], John A. McGrath[6], Jemima E. Mellerio[6], Johann W. Bauer[3], and Andrew P. South[1]

Abstract

Purpose: Squamous cell carcinoma (SCC) of the skin is the leading cause of death in patients with the severe generalized form of the genetic disease recessive dystrophic epidermolysis bullosa (RDEB). Although emerging data are identifying why patients suffer this fatal complication, therapies for treatment of RDEB SCC are in urgent need.

Experimental Design: We previously identified polo-like kinase 1 (PLK1) as a therapeutic target in skin SCC, including RDEB SCC. Here, we undertake a screen of 6 compounds originally designated as PLK1 inhibitors, and detail the efficacy of the lead compound, the multipathway allosteric inhibitor ON-01910, for targeting RDEB SCC *in vitro* and *in vivo*.

Results: ON-01910 (or rigosertib) exhibited significant specificity for RDEB SCC: in culture rigosertib induced apoptosis in 10 of 10 RDEB SCC keratinocyte populations while only slowing the growth of normal primary skin cells at doses 2 orders of magnitude higher. Furthermore, rigosertib significantly inhibited the growth of two RDEB SCC in murine xenograft studies with no apparent toxicity. Mechanistically, rigosertib has been shown to inhibit multiple signaling pathways. Comparison of PLK1 siRNA with MEK inhibition, AKT inhibition, and the microtubule-disrupting agent vinblastine in RDEB SCC shows that only PLK1 reduction exhibits a similar sensitivity profile to rigosertib.

Conclusions: These data support a "first in RDEB" phase II clinical trial of rigosertib to assess tumor targeting in patients with late stage, metastatic, and/or unresectable SCC.

Introduction

Patients with the devastating inherited skin disease recessive dystrophic epidermolysis bullosa (RDEB) are at significantly increased risk of developing aggressive cutaneous squamous cell carcinoma (SCC), which is the cause of death by age 45 years in 70% of individuals with the severe generalized form of the disease (1, 2). Furthermore, 5-year survival in all RDEB subtypes diagnosed with SCC is close to 0% (2), making RDEB SCC one of the most aggressive forms of this tumor type. Current clinical guidelines offer limited treatment options for RDEB SCC and consist of wide local excision, radiotherapy, and in late stages, limb amputation (3). New approaches to therapy for RDEB SCC are in urgent need.

RDEB is caused by mutations in *COL7A1*, the gene encoding type VII collagen (4). However, *COL7A1* does not behave as a classical tumor suppressor as heterozygous carriers are not at increased risk of skin cancer and *COL7A1* has not been identified as a significantly mutated gene in genetic profiling of any tumor type to date. RDEB is characterized by skin fragility, trauma-induced skin blistering, and chronic nonhealing wounds (5), and work by us and others has implicated the tumor microenvironment as a driving mechanism of cancer development (6, 7). Our recent comprehensive genetic characterization of RDEB SCC demonstrates that these tumors are driven by somatic mutation in driver genes that are identical to UV-induced skin SCC and head and neck SCC (HNSCC; ref. 8), and we have consistently been unable to identify genetic mechanisms which explain the aggressive nature of RDEB SCC (9, 10). Our early microarray gene expression profiling failed to significantly differentiate RDEB

[1]Department of Dermatology and Cutaneous Biology, Thomas Jefferson University, Philadelphia, Pennsylvania. [2]Division of Cellular Medicine, University of Dundee, Dundee, United Kingdom. [3]EB House Austria, Research Program for Molecular Therapy of Genodermatoses, Department of Dermatology, University Hospital of the Paracelsus Medical University Salzburg, Austria. [4]Fundación DEBRA Chile, Santiago, Chile. [5]Centro de Genética y Genómica, Facultad de Medicina Clínica Alemana, Universidad del Desarrollo, Santiago, Chile. [6]St. John's Institute of Dermatology, King's College London (Guy's Campus), London, United Kingdom. [7]Department of Dermatology, Medical Center–University of Freiburg, Faculty of Medicine, Freiburg, Germany. [8]Instituto Dearmatologico de Jalisco, Guadalajara, Mexico. [9]Facultad de Medicina Clínica Alemana, Universidad del Desarrollo, Santiago, Chile. [10]INSERM UMR 1163, Paris, France. [11]Imagine Institute, Paris, France.

Note: Supplementary data for this article are available at Clinical Cancer Research Online (http://clincancerres.aacrjournals.org/).

V.S. Atanasova and C. Pourreyron contributed equally to this article.

Corresponding Author: Andrew P. South, Thomas Jefferson University, 233 S. 10th Street, BLSB 406, Philadelphia, PA 19107. Phone: 215-955-1934; Fax: 215-503-5788; E-mail: Andrew.south@Jefferson.edu

Clin Cancer Res 2019;25:3384–91

doi: 10.1158/1078-0432.CCR-18-2661

Translational Relevance

Collectively, our data support a clinical trial of rigosertib for treatment of recessive dystrophic epidermolysis bullosa–associated squamous cell carcinoma, an inherently aggressive subtype of squamous cell carcinoma with extremely low 5-year survival. Currently, there are no effective treatments for this devastating cancer, and often times, initial squamous cell carcinoma will recur and readily metastasize; any effective systemic therapy that reduces tumor burden will improve quality of life in this patient population.

from skin SCC in cultured keratinocytes (10). However, this work did identify polo-like kinase 1 (PLK1) as a therapeutic target in RDEB SCC. Here, we follow up this finding with a screen of compounds originally designated as PLK1 inhibitors and identify ON-01910, or rigosertib, as a lead candidate for therapy in RDEB SCC.

Materials and Methods

Cell cultures

Cells were isolated from biopsies taken as part of routine surgical or diagnostic procedures. Informed written consent was obtained from each patient or in the case of underaged children from their parents or guardian. Ethical approval for this investigation was obtained from all local ethics committees, and this study was performed in accordance with the Helsinki declaration. All cells were isolated as described (11) and cultured at 37°C in 5% CO_2. Keratinocytes were grown in DMEM (Corning cellgro, Mediatech Inc.)/Ham's F12 medium (3:1), supplemented with 10% FBS (PEAK Serum, Cat PS-FB1), 10 ng/mL of EGF, 10^{-10} mol/L cholera toxin, 0.4 μg/mL of hydrocortisone, 5 μg/mL of transferrin, 5 μg/mL of insulin, and 13 ng/mL liothyronine. Supplementary Table S1 details all cells used in this study. All cells are routinely tested for *Mycoplasma* using either a PCR approach or a colorimetric detection assay (MycoAlert, Lonza). SCCRDEB2, SCCRDEB3, SCCRDEB70, RDEB84, and RDEB86 were *Mycoplasma* positive upon isolation and were treated with Plasmocure (InvivoGen). Only cells which yielded a negative *Mycoplasma* test were used in the assays described.

Protein quantification

Total lysates were quantified using Pierce bicinchoninic assay Protein Assay kit (Fisher Scientific, Cat. # 23225), and 5 to 50 μg of protein were loaded onto SDS-PAGE gel. The signal from Western blot analysis was quantified with Image J. P-CRAF and P-AKT were quantified relative to GAPDH.

Drug treatment and Western blot analysis

Rigosertib (ON 01910.Na) was either purchased from Selleckchem.com or provided by Onconova Therapeutics, Inc. All other drugs were purchased from Selleckchem.com. Note that 2 to 4 × 10^5 keratinocytes were plated in a 6-well dish. On the following day, the medium was changed with the drug at 1 μmol/L or vehicle control. Medium was left for 48 hours, and cells were lysed with radioimmunoprecipitation assay buffer. Lysate was placed in a centrifuge for 5 minutes at 4°C, and the supernatant was mixed with a 6x Laemmli loading buffer. Samples were boiled for 5 minutes at 95°C before being loaded onto SDS-PAGE gels. Primary antibodies used were PLK1 (Cell Signaling Technology, 208G4), CRAF polyclonal (Cell Signaling Technology, 9422S), P-CRAF (Cell Signaling Technology, 9427S), P-AKT (Cell Signaling Technology, 9271), AKT (Cell Signaling Technology, 9272), and GAPDH (Santa Cruz Biotechnology, 6C5). Resolved proteins were transferred onto nitrocellulose membrane with a BioRad Trans-Blot-Turbo (Bio-Rad), blocked in TBS-0.1% Tween-20 with 5% milk or 5% BSA according to requirements of the primary antibody, and incubated overnight with the primary antibody. After incubation with IgG-HRP–conjugated secondary antibody (Santa Cruz Biotechnology), membrane was incubated with Pierce ECL Western blotting substrate (Fisher Scientific) and exposed to CL-XPosure X-ray film (Fisher Scientific).

Immunofluorescence

RDEB SCC and human control skin biopsies were frozen in optimal cutting temperature (Sakura Finetek USA) and cut at 6 μm on a cryostat. Sections were fixed with 50:50 methanol: acetone mixture for 5 minutes. Slides were rinsed with 1x PBS and permeabilized with PBS/0.1% Tween-20 (Sigma Aldrich) for 5 minutes followed by blocking for 1 hour with PBST/3% BSA (Sigma Aldrich). Primary antibodies were incubated for 1.5 hours at room temperature. Secondary antibody Alexa Fluor 594 goat anti-rabbit (1:800, Molecular Probes) was applied for 1 hour at room temperature. Slides were cover-slipped with hard set 4,6-diamidino-2-phenylindole (DAPI; Vector Labs) and examined by fluorescence microscopy (EVOS FL cell imaging system, ThermoFisher).

Cell growth and metabolism assays

Colorimetric assays of mitochondrial dehydrogenase activity were performed using the MTS CellTitre 96 AQueous One Solution Cell Proliferation Assay (Promega) according to the manufacturer's instructions. In each case, 1 to 4 × 10^4 cells were seeded into replica 96-well plates, and readings were taken at intervals up to a maximum of 96 hours. We have previously shown that an increase in mitochondrial dehydrogenase activity using this assay directly correlates with primary non-SCC and SCC cell number determined using a CASY Model TT cell counter (Roche Diagnostics Ltd.; ref. 10).

For crystal violet assay of cell growth, 1 to 4 × 10^4 cells were seeded into replica 96-well plates and fixed with 70% ETOH at intervals up to a maximum of 96 hours. After fixation, wells were incubated with a solution of 0.2% crystal violet in 2% ETOH for 1 hour at room temperature followed by three washes with tap water. Plates were allowed to air dry and were then photographed, and 100 μL of 70% ETOH was added to each well for 20 minutes, the plate was agitated to homogenize the solution, and the absorbance at 595 nm was measured using a plate reader (Flexstation 3, Molecular Devices). For photographic quantification, black and white images were produced using the threshold function in Adobe Photoshop C6 (Adobe) and quantified using the measure tool.

Cell-cycle analysis

5-Bromodeoxyuridine (BrdU; Sigma-Aldrich) was added to cells at 30 mmol/L final concentration for 2 hours. Cells were collected and washed in PBS and then fixed overnight in cold 70% ETOH. RNase A (Sigma) was added at 100 μg/mL, in 5%

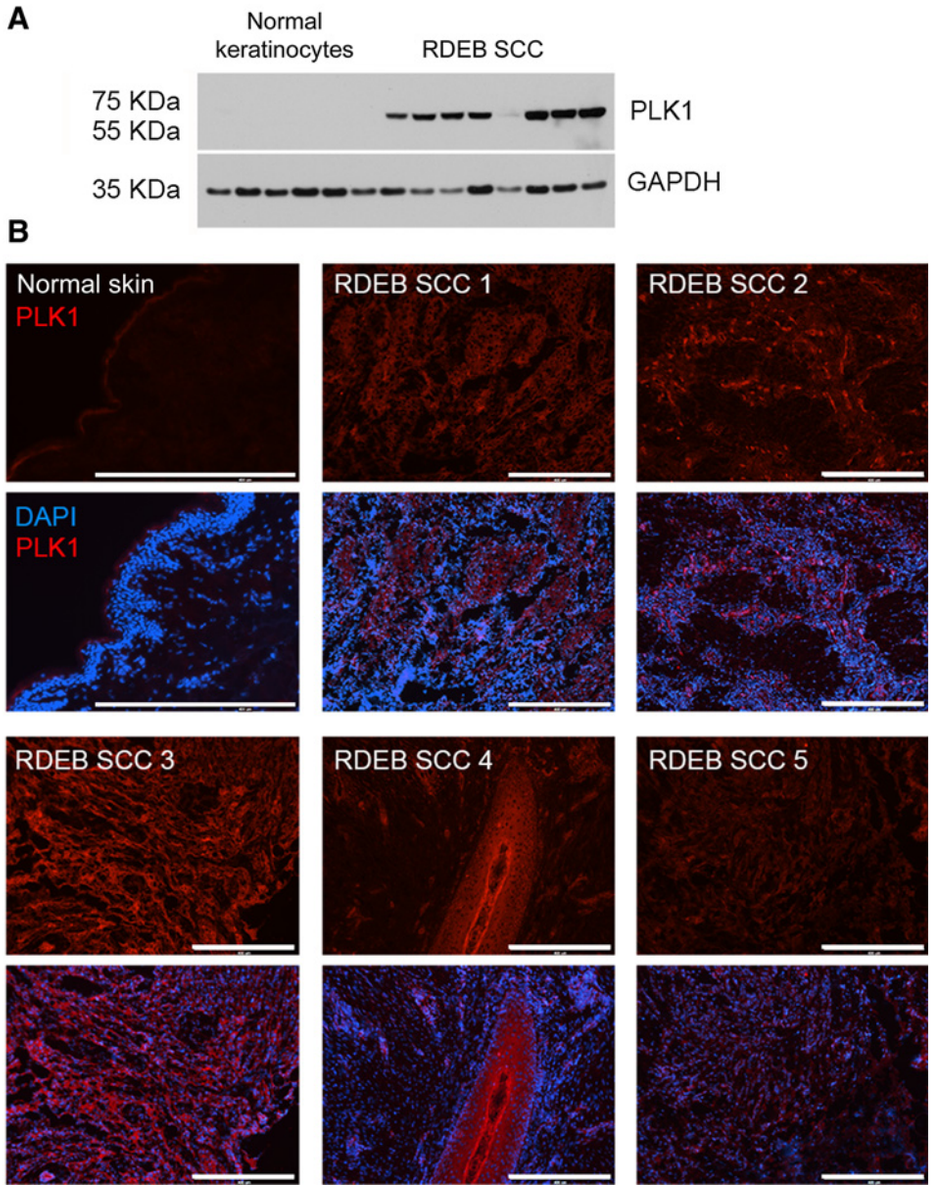

Figure 1.
PLK1 is increased in RDEB SCC. **A,** 5 μg of total cell lysate was resolved on a 6% SDS PAGE gel, transferred to nitrocellulose membrane before being incubated with antibodies raised against PLK1 (Cell Signaling Technology, 208G4) and GAPDH (Santa Cruz Biotechnology, 6C5). Samples loaded from left to right: lanes 1–2 = normal primary breast keratinocytes (Br61, Br63), lanes 3–6 = RDEB primary keratinocytes (RDEB81, RDEB84, RDEB85, and RDEB118), lanes 7–14 = RDEB SCC keratinocytes (SCCRDEB108, SCCRDEB2, SCCRDEB3, SCCRDEB70, SCCRDEB71, SCCRDEB4, SCCRDEB62, and SCCRDEB106). **B,** 6 μm frozen sections were processed and incubated with an antibody raised against PLK1 (Sigma-Aldrich, HPA053229, red) as well as the nuclear stain DAPI (blue). Bar, 400 μm.

Tween-20 and PBS for 30 minutes at 37°C. Pepsin (Sigma) was added at 1 mg/mL in 30 mmol/L HCL for 30 minutes at 37°C, and DNA was denatured with 2N HCl containing 0.5% Tween-20 in PBS for 30 minutes at 37°C. An anti-BrdU antibody (Invitrogen) diluted in PBS/0.1% Tween/1% BSA was added for 2 hours followed by a wash with 1% BSA. After passing the cells through a 70 μm filter, propidium iodide (Sigma) was added in the final wash step at a concentration of 25 mg/mL. Samples were analyzed using a FACScan flow cytometer and CellQuest software (Becton Dickinson).

Apoptosis ELISA

Apoptosis was measured using the Cell Death Detection ELISA^{PLUS} (ROCHE, Cat. # 11774425001). Briefly, non-SCC keratinocytes were plated at 5×10^3 cells/well and SCC keratinocytes at 2.5×10^4 cells/well in 96-well plates. On the next day, the cells were treated with the drug (1 μmol/L) for 16 to 24 hours. Cells were lysed for 30 minutes, and 20 μL of the lysate was incubated with 80 μL immunoreagent. After incubation, the reaction was stopped with ABTS solution, and absorbance was read using a plate reader at 405 nm and 490 nm (Flexstation 3, Molecular Devices).

siRNA knockdown

siRNA oligonucleotides targeting PLK1 (FlexiTube siRNA, Qiagen, Cat. #: 1027416), a negative scrambled control (AllStars Negative Control siRNA, Qiagen, Cat. #: SI03650318), and a positive cell death control (AllStars Hs Cell Death siRNA, Qiagen, Cat. #: SI04381048) were used. Cells were seeded in 6-well plates at 2.5×10^5 cells/well and 24 hours later transfected with siRNA (40 nmol/L final concentration) using Lipofectamine 2000 (Invitrogen) diluted in Opti-MEM (Invitrogen) according to the

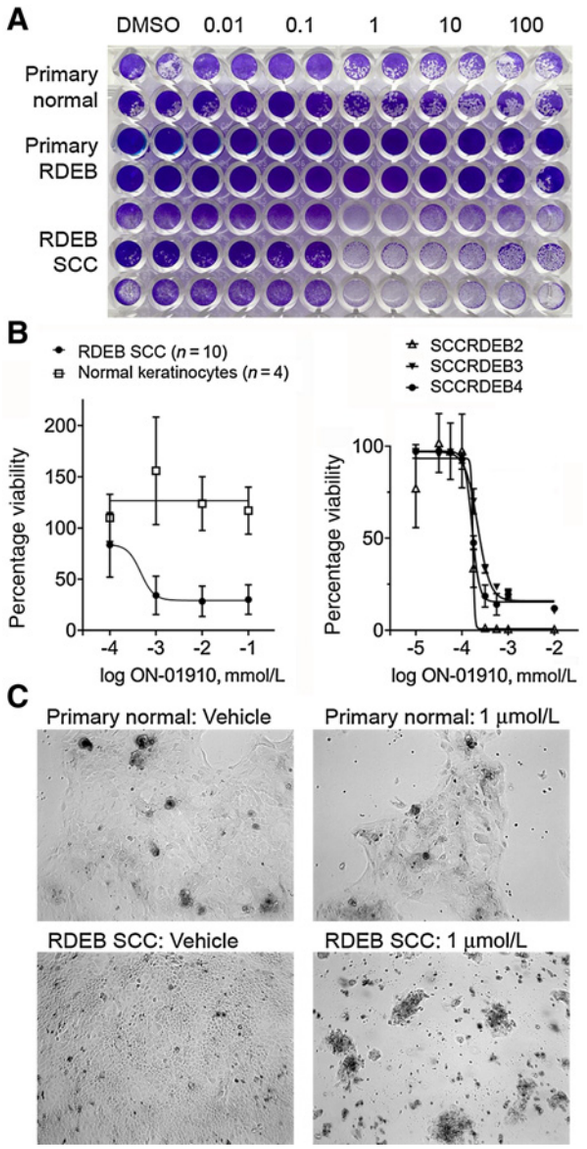

Figure 2.

Rigosertib effectively targets RDEB SCC keratinocytes *in vitro*. **A,** Normal primary keratinocytes (FS1, Br61), RDEB primary keratinocytes (RDEB81, RDEB84), and RDEB SCC keratinocytes (SCCRDEB2, SCCRDEB3, and SCCRDEB4) were seeded into wells of a 96-well plate and exposed to vehicle (DMSO) or increasing concentrations of rigosertib (0.01–100 µmol/L) for 48 hours. Cells were then fixed with 70% ETOH and incubated with the cell dye crystal violet. Plate was photographed after excess dye was washed away with water. **B,** Crystal violet retention was measured using a spectrometer, and values relative to vehicle alone were calculated for cells exposed to increasing concentrations of rigosertib. Left graph shows response curve (±SD) from a single experiment using 4 populations of primary non-SCC keratinocytes (Br61, Br63, RDEB81, and RDEB84) and 10 populations of RDEB SCC keratinocytes. Right graph shows results for RDEB SCC cells shown in **A** after exposure to a wider range of drug concentrations used to determine EC_{50} values for all 10 populations of RDEB SCC keratinocytes (see Table 1 and Supplementary Fig. S1). **C,** Cells were plated into a 6-well plate and incubated with vehicle alone or 1 µmol/L of rigosertib for 48 hours before photographs were taken. Br63 (Primary normal) and SCCRDEB3 cells are shown.

manufacturer's instructions. Cells were left for 16 to 24 hours before being lysed for Western blotting or trypsinized and seeded in 96-well plates at 5×10^3 cells/well in 100 µL of media. For comparison of siRNA with vinblastine, cells were seeded directly in 96-well plates at 1×10^4 cells/well in 100 µL of media and transfected 24 hours later as described.

In vivo tumor growth and treatment

All animal experiments were conducted in accordance with UK Home Office (Project License # 60/4054) and Thomas Jefferson IACUC (Protocol # 01719) regulations. For tumorigenicity assays, a suspension of 1 to 4×10^6 tumor cells was mixed with high-concentration Matrigel (Becton Dickinson) and injected subcutaneously into the flanks of adult female SCID Balb/c mice (between 6 and 12 weeks of age and 18–27 g in weight) purchased from The Jackson Laboratories (stock # 001803) or from Taconic (model # CB17SC). Tumors were measured by a caliper, and treatment began when volume reached 100 to 200 mm^3. Animals were treated with 20 mg/kg rigosertib dissolved in PBS, and animals were distributed into treatment or vehicle control groups by alternating between treatment (first animal to reach minimum 100 mm^3) and vehicle control (second animal). For the experiment shown in Supplementary Fig. S1, 25 mice were injected with 4×10^6 SCCRDEB16 cells, and BI-2536 treatment was included as a positive control for 2 animals where every third animal was allocated to this group. For the experiment shown in Fig. 5, 20 mice were injected with 1×10^6 SCCRDEB106 cells. In all cases, animals where tumors were attached to the rib-cage or growing superficially were sacrificed and not included in the experiment.

Terminal deoxynucleotidyl transferase dUTP nick end labeling analysis

Terminal deoxynucleotidyl transferase dUTP nick end labeling (TUNEL) was performed using the TACS2 TdT_Fluor In Situ Apoptosis Detection kit (Trevigen) according to the manufacturer's instructions. Slides were fixed with mounting medium containing DAPI and were viewed under a fluorescence microscope using a 495 nm filter.

Statistical analysis

Paired two-tailed *t* test was used for statistical analysis using Prism 8 (GraphPad Software). EC_{50} values were calculated with nonlinear regression using Prism 8.

Results

PLK1 is increased in RDEB SCC

We previously identified PLK1 mRNA was increase in 4 RDEB SCC keratinocyte cultures compared with normal primary keratinocyte controls (10). Here, we extend this observation to a total of 10 separate SCC populations and identify PLK1 increased in 10 of 10 fresh-frozen RDEB SCC tissue samples using IHC (Fig. 1).

ON-01910 emerges with the largest delta comparing growth in RDEB SCC and primary skin cells

After confirmation of increased PLK1 in all RDEB SCC assessed, we set out to compare the efficacy of commercially available PLK1 inhibitors for targeting RDEB SCC. We initially assessed the effects of 6 PLK1 inhibitors on cell metabolism using an MTS assay after 48-hour exposure to normal primary keratinocytes ($n = 1$), RDEB primary fibroblasts ($n = 4$), and RDEB SCC keratinocytes ($n = 4$;

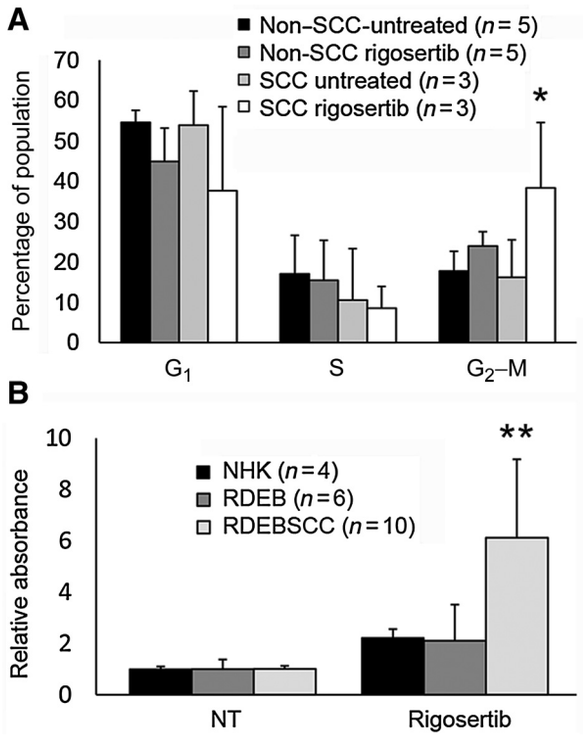

Figure 3.

Rigosertib induces G_2–M arrest and apoptosis in RDEB SCC keratinocytes. **A,** Cell-cycle analysis in either RDEB SCC keratinocytes (SCCRDEB2, SCCRDEB3, SCCRDEB4, SCCRDEB53, and SCCRDEB106) or non-SCC keratinocytes (Br61, RDEB115, and RDEB124) treated with rigosertib (1 μmol/L, non–SCC-treated and SCC-treated) or vehicle control (non–SCC-untreated and SCC-untreated), and stained for BrdU and propidium iodide. Results expressed as percentage of cells at the G_0–G_1, S, and G_2–M phases of cell cycle 16 hours following treatment. The results shown are the mean (±SD). **B,** Graph shows relative mean absorbance increase using a colorimetric assay to detect cleaved nucleosomes in the cytoplasm as a measure of apoptosis after exposure of cells to vehicle or rigosertib. Data shown are the mean (±SD) from two independent experiments using 2 populations of normal primary keratinocytes (Br46 and Br61), 3 populations of primary RDEB keratinocytes (RDEB81, RDEB84, and RDEB86), and 10 populations of RDEB SCC keratinocytes (Supplementary Table S1) exposed to 1 μmol/L of rigosertib for 16 to 24 hours. *, $P < 0.05$ and **, $P < 0.005$ (Student *t* test).

Supplementary Table S2). These data identified the compound ON-01910, also known as rigosertib, as having the greatest specificity for RDEB SCC keratinocytes when compared with normal primary keratinocytes and RDEB primary fibroblasts (Supplementary Table S2).

Next, these data were confirmed in all 10 separate patient-derived RDEB SCC cell lines using crystal violet uptake by live cells after 48- 72-hour exposure to varying drug concentrations (Fig. 2A and B; Supplementary Fig. S1). These data identified clear specificity for RDEB SCC keratinocytes when compared with primary normal or primary non-SCC RDEB keratinocytes. We also observed that whereas higher concentrations of rigosertib could inhibit the growth of non-SCC primary keratinocytes in culture (both RDEB and non-RDEB, Fig. 2A and B), no obvious signs of cell death were evident while in RDEB SCC keratinocyte populations cell death was widespread (Fig. 2C).

ON-01910 induces apoptosis in RDEB SCC keratinocytes

In agreement with our previous data using PLK1 siRNA and the PLK1 inhibitors BI-2536 and GW-843682 (10), as well as published studies of rigosertib (12–14), exposure of RDEB SCC keratinocytes to rigosertib induced cell-cycle arrest and apoptosis (Fig. 3A and B).

PLK1 siRNA knockdown mimics ON-01910 specificity in RDEB SCC keratinocytes

Since its identification as an inhibitor of PLK1, rigosertib has been shown to inhibit a variety of kinases, including AKT (12), and recently rigosertib has been shown to compete with activated RAS for binding to CRAF (15). More recently rigosertib was shown to bind to and destabilize microtubules (16), and studies in other malignancies have shown synthetic lethality of PLK1 and microtubule-destabilizing agents (17).

To investigate potential mechanisms of action of rigosertib, we first exposed RDEB SCC keratinocytes to inhibitors of MEK and AKT as well as the microtubule-destabilizing agent vinblastine. These data showed some efficacy of MEK inhibition at lower concentrations but no specificity over normal cells at higher doses, no apparent effect of AKT inhibition and differential selectivity of vinblastine (Fig. 4A). Next, we performed siRNA knockdown of PLK1 and showed inhibition of cell growth in all RDEB SCC populations tested (Fig. 4B). Four of the populations showed only moderate growth inhibition after PLK1 siRNA (45%–75%), and in these cells, we performed siRNA knockdown in the presence of vinblastine but failed to see any overt synergy (Fig. 4C) as has previously been reported in rhabdomyosarcoma (17). Treatment of RDEB SCC keratinocytes with rigosertib inhibited phosphorylation of both AKT and CRAF which was also evident after PLK1 siRNA knockdown (Supplementary Fig. S2).

ON-01910 effectively targets RDEB SCC keratinocytes *in vivo*

Finally, we sought to establish the ability of rigosertib to target RDEB SCC keratinocytes *in vivo*. Tumor xenograft models showed that either local tumor injection (Supplementary Fig. S3) or systemic delivery (Fig. 5) effectively inhibited the growth of two separate RDEB SCC keratinocyte cell lines *in vivo*. Ki-67 and TUNEL IHC showed that tumors harvested from those animals treated with rigosertib had significantly fewer proliferative tumor cells and significantly more apoptosis than vehicle control-treated animals (Fig. 5D and E). Unlike our experiments with BI-2536 (Supplementary Fig. S3 and ref. 10), we did not see any erythema or ulceration of tissue associated with the injection site when using rigosertib.

Discussion

SCC is a lethal complication for the majority of patients with the already devastating genetic disease RDEB, and currently, there are no approved or effective therapies for SCC in this patient population (3). Here, we present evidence that the multikinase inhibitor rigosertib effectively induces apoptosis in 10 of 10 separate RDEB SCC populations and targets *in vivo* tumor growth in xenograft studies, data which support a clinical trial of rigosertib in RDEB SCC. In particular, the lack of significant targeting of nontumor cells by rigosertib (Fig. 2), the lack of any observed toxicity in our animal studies coupled with the overall favorable side-effect profile for this drug as determined by trials in patients with myelodysplastic syndrome (18) supports the notion that

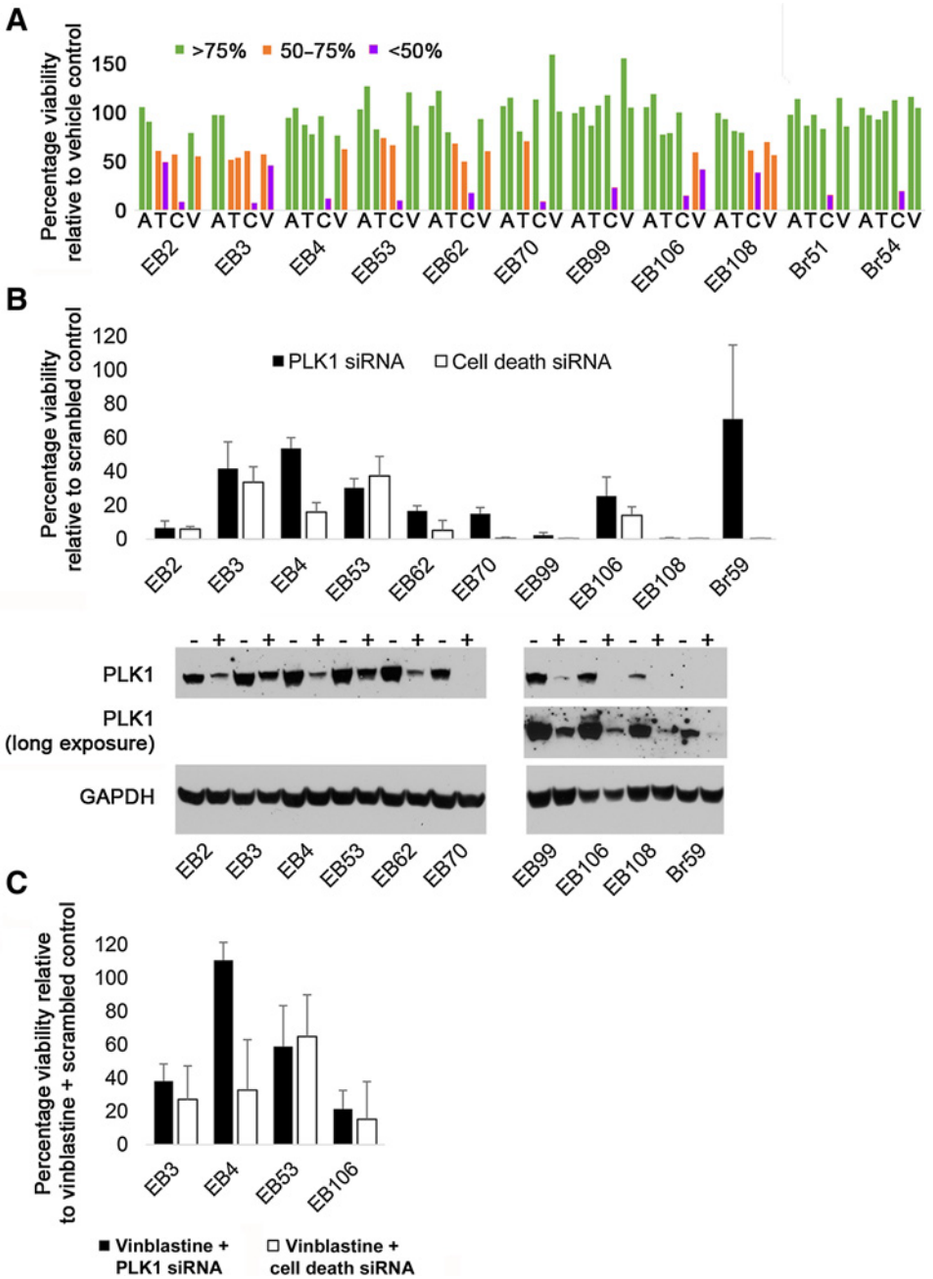

Figure 4.
Rigosertib specificity mirrors PLK1 siRNA knockdown in RDEB SCC keratinocytes. RDEB SCC keratinocytes ($n = 9$) were exposed to AKT and MEK inhibitors, the microtubule-disrupting agent vinblastine and PLK1 siRNA knockdown. **A,** Cells were seeded into wells of a 96-well plate and exposed to vehicle (DMSO) or drug for 48 hours. Cells were then fixed with 70% ETOH, and crystal violet retention was measured using a spectrometer, and values relative to vehicle alone (100%) were plotted. For each cell line, bars indicate the following, left to right: A = AKT inhibitor LY294002 0.1 μmol/L and 5 μmol/L, T = trametinib 0.1 μmol/L and 1 μmol/L, C = cobimetinib 2 μmol/L and 5 μmol/L, V = vinblastine 0.1 μmol/L and 5 μmol/L. **B,** Cells were seeded into wells of duplicate 6-well plates and transfected with PLK1 siRNA, scrambled control, or a cell death control siRNA. Sixteen hours later, one set of cells was trypsinized and transferred to 96-well plates before being fixed 48 hours later. Total cell lysates were isolated from duplicate 6-well plates at the same time as the 96-well reseeded plates were fixed. Graph shows cell growth relative to scrambled control siRNA after staining with crystal violet, whereas images below show immunoblotting results with antibodies raised against PLK1 (Cell Signaling Technology, 208G4) and GAPDH (Santa Cruz Biotechnology, 6C5). +, PLK1 siRNA and −, scrambled control siRNA. **C,** Cells were seeded directly into wells of a 96-well plate and transfected with PLK1 siRNA, scrambled control, or a cell death control siRNA. Sixteen hours later, cells were treated with 1 μmol/L vinblastine before being fixed 48 hours later. Graph shows cell growth relative to scrambled control siRNA after staining with crystal violet.

even in a patient group such as RDEB, where numerous clinical complications abound as a result of lack of mechanical integrity of the epidermis, rigosertib may be well tolerated.

Previous studies of rigosertib in the context of HNSCC have demonstrated similar efficacy in a subset of tumor cell lines/populations (19). The data presented in our study show remarkable sensitivity of RDEB SCC to rigosertib and suggest that this subtype of SCC may respond to rigosertib treatment more favorably. We have recently increased our current understanding of RDEB SCC through comprehensive genomic characterization of 27 tumors, including 9 of 10 cell lines described here (8), which shows that other than mutation burden and mechanism, the somatic mutation profile in RDEB SCC is no different to HNSCC or UV-induced skin SCC, and that RDEB SCC are most similar to the basal and mesenchymal subtypes of HNSCC at the level of transcriptomics (8). This similarity to subtypes of HNSCC at the level of mRNA expression may begin to offer opportunity for identifying biomarkers of drug sensitivity, and we are actively pursuing this line of inquiry. Another feature identified in RDEB SCC is homogeneity at the level of somatic tumor driver-gene mutation (8), and this may be advantageous in the context of targeted therapies where resistance that often develops is associated with genetic heterogeneity (20).

With regard to mechanism of action of rigosertib in RDEB SCC, we have investigated pathways reported to be targeted by rigosertib and showed that only siRNA knockdown of PLK1 has a

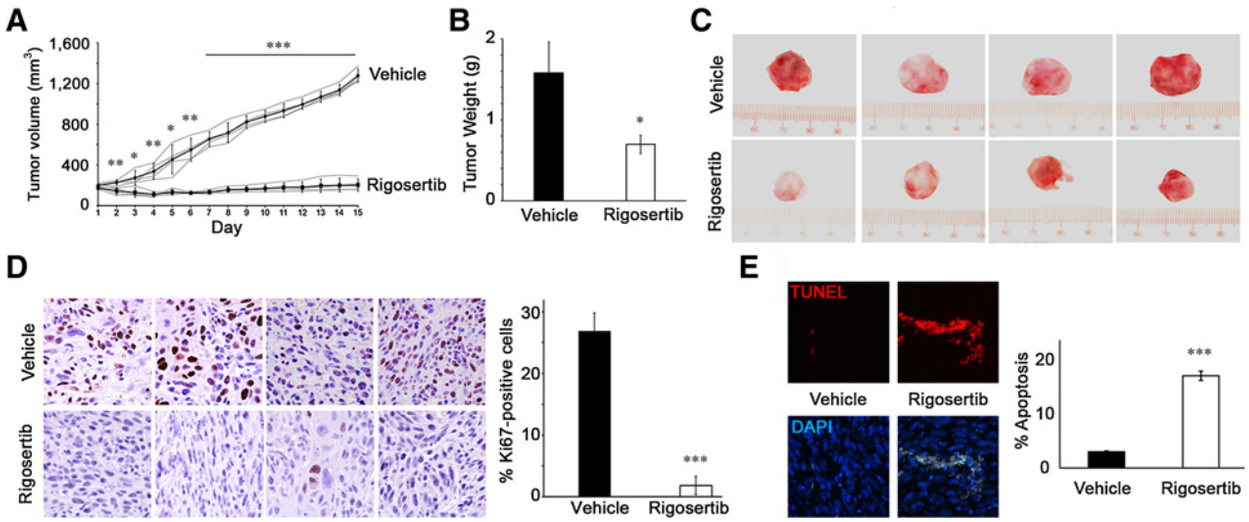

Figure 5.

Rigosertib effectively targets RDEB SCC keratinocytes *in vivo*. Animals bearing SCCRDEB106 xenograft tumors that had reached >100 mm^3 were treated with either rigosertib ($n = 4$) or vehicle control ($n = 4$) injected i.p. every day for 14 days. Tumors were measured with calipers (**A**) until day 15 when animals were sacrificed, tumors were harvested, weighed (**B**), and photographed (**C**) before being bisected and frozen or fixed with formalin and paraffin embedded. **D,** 4 μm FFPE sections were cut and incubated with an antibody recognizing Ki-67 (Abcam, ab16667, 1:200) as well as the nuclear stain hematoxylin. Graph shows the number of Ki-67–positive nuclei manually counted from five distinct microscopic fields for each tumor ($n = 8$) at 200× magnification. **E,** 4 μm FFPE sections were cut and incubated with an antibody recognizing TUNEL (Trevigen) as well as the nuclear stain DAPI. Graph shows the number of TUNEL-positive nuclei per cell calculated using ImageJ software. *, $P < 0.05$; **, $P < 0.01$; and ***, $P < 0.001$ (Student *t* test).

similar profile in targeting all RDEB SCC cell lines with little effect to normal cells (Fig. 4). However, the level of PLK1 expression did not seem to show any clear correlation with the sensitivity of individual RDEB SCC cell lines to either PLK1 siRNA or rigosertib, which does not rule out contribution of another pathway when considering RDEB SCC sensitivity to rigosertib over normal cells. Further understanding of this sensitivity may offer precision medicine opportunities for use of rigosertib in subsets of sporadic SCC arising at different anatomical locations, and future work will concentrate on understanding the relationship between apoptosis induction and either PLK1 siRNA or rigosertib exposure in RDEB SCC.

Finally, the data described here have supported the approval of a clinical trial comparing the tolerability and efficacy of rigosertib in RDEB SCC (ClinicalTrials.gov Identifier: NCT03786237), and we aim to analyze patient response in the context of biomarker expression, tumor and patient genotype, as well as sensitivity of patient material in the laboratory.

Table 1. EC_{50} (μmol/L) values as determined by crystal violet assay for 10 RDEB SCC cell lines

Cell line	μmol/L
SCCRDEB2	0.1731
SCCRDEB3	0.2198
SCCRDEB4	0.1647
SCCRDEB53	1.567
SCCRDEB62	0.1977
SCCRDEB70	0.1741
SCCRDEB71	0.2165
SCCRDEB99	0.2197
SCCRDEB106	0.1496
SCCRDEB108	0.0834

Disclosure of Potential Conflicts of Interest

J.W. Bauer reports receiving speakers bureau honoraria from and is a consultant/advisory board member for Castle Creek Pharma, and holds ownership interest (including patents) in Diaderm. No potential conflicts of interest were disclosed by the other authors.

Authors' Contributions

Conception and design: A.P. South

Development of methodology: V.S. Atanasova, C. Pourreyron, M. Farshchian, C.A. Brown IV, J.C. Salas-Alanis, J.W. Bauer, A.P. South

Acquisition of data (provided animals, acquired and managed patients, provided facilities, etc.): C. Pourreyron, M. Farshchian, M. Lawler, C.A. Brown IV, S. Wright, M. Warkala, I. Fuentes, M. Prisco, E. Rashidghamat, C. Has, J.C. Salas-Alanis, F. Palisson, A. Hovnanian, J.A. McGrath, J.E. Mellerio, J.W. Bauer, A.P. South

Analysis and interpretation of data (e.g., statistical analysis, biostatistics, computational analysis): V.S. Atanasova, M. Farshchian, M. Lawler, C.A. Brown IV, S. Wright, M. Warkala, I. Fuentes, A.P. South

Writing, review, and/or revision of the manuscript: C. Pourreyron, M. Farshchian, C.A. Brown IV, S. Wright, I. Fuentes, M. Prisco, E. Rashidghamat, C. Has, J.C. Salas-Alanis, A. Hovnanian, J.A. McGrath, J.E. Mellerio, J.W. Bauer, A.P. South

Administrative, technical, or material support (i.e., reporting or organizing data, constructing databases): V.S. Atanasova, S.A. Watt, C. Guttmann-Gruber, J. Piñón Hofbauer, A.P. South

Study supervision: A.P. South

Other (performed experiments): V.S. Atanasova

Acknowledgments

This work was supported by DEBRA International—funded by DEBRA UK (grants to A.P. South, and to A.P. South, J.W. Bauer, and J.E. Mellerio) and the Office of the Assistant Secretary of Defense for Health Affairs and the Defense Health Agency J9, Research and Development Directorate, through the Congressionally Directed Medical Research Program under Award No. W81XWH-18-1-0382 (to A.P. South). Opinions, interpretations, conclusions, and recommendations are those of the authors and are not necessarily endorsed by the

Department of Defense. M. Farshchian is supported by the Sigrid Juselius Foundation, Orion Research Foundation, and the Finnish Society of Dermatology. We would like to thank all the patients who contributed to this study, Evan Greenawalt for technical assistance and the Flow Cytometry Shared Resource at the Sidney Kimmel Cancer Center, supported by the NCI, grant 5P30CA056036-17.

The costs of publication of this article were defrayed in part by the payment of page charges. This article must therefore be hereby marked *advertisement* in accordance with 18 U.S.C. Section 1734 solely to indicate this fact.

Received August 15, 2018; revised January 11, 2019; accepted February 21, 2019; published first March 7, 2019.

References

1. Fine JD, Bruckner-Tuderman L, Eady RA, Bauer EA, Bauer JW, Has C, et al. Inherited epidermolysis bullosa: updated recommendations on diagnosis and classification. J Am Acad Dermatol 2014;70:1103–26.
2. Fine JD, Johnson LB, Weiner M, Li KP, Suchindran C. Epidermolysis bullosa and the risk of life-threatening cancers: the National EB Registry experience, 1986–2006. J Am Acad Dermatol 2009;60:203–11.
3. Mellerio JE, Robertson SJ, Bernardis C, Diem A, Fine JD, George R, et al. Management of cutaneous squamous cell carcinoma in patients with epidermolysis bullosa: best clinical practice guidelines. Br J Dermatol 2016;174:56–67.
4. Christiano AM, Greenspan DS, Hoffman GG, Zhang X, Tamai Y, Lin AN, et al. A missense mutation in type VII collagen in two affected siblings with recessive dystrophic epidermolysis bullosa. Nat Genet 1993;4:62–6.
5. Mellerio JE, Weiner M, Denyer JE, Pillay EI, Lucky AW, Bruckner A, et al. Medical management of epidermolysis bullosa: proceedings of the IInd international symposium on epidermolysis bullosa, Santiago, Chile, 2005. Int J Dermatol 2007;46:795–800.
6. Ng YZ, Pourreyron C, Salas-Alanis JC, Dayal JH, Cepeda-Valdes R, Yan W, et al. Fibroblast-derived dermal matrix drives development of aggressive cutaneous squamous cell carcinoma in patients with recessive dystrophic epidermolysis bullosa. Cancer Res 2012;72:3522–34.
7. Mittapalli VR, Madl J, Loffek S, Kiritsi D, Kern JS, Romer W, et al. Injury-driven stiffening of the dermis expedites skin carcinoma progression. Cancer Res 2016;76:940–51.
8. Cho RJ, Alexandrov LB, den Breems NY, Atanasova VS, Farshchian M, Purdom E, et al. APOBEC mutation drives early-onset squamous cell carcinomas in recessive dystrophic epidermolysis bullosa. Sci. Trans. Med 2018;10:eaas9668.
9. Purdie KJ, Pourreyron C, Fassihi H, Cepeda-Valdes R, Frew JW, Volz A, et al. No evidence that human papillomavirus is responsible for the aggressive nature of recessive dystrophic epidermolysis bullosa-associated squamous cell carcinoma. J Invest Dermatol 2010;130:2853–5.
10. Watt SA, Pourreyron C, Purdie K, Hogan C, Cole CL, Foster N, et al. Integrative mRNA profiling comparing cultured primary cells with clinical samples reveals PLK1 and C20orf20 as therapeutic targets in cutaneous squamous cell carcinoma. Oncogene 2011;30:4666–77.
11. Purdie KJ, Pourreyron C, South AP. Isolation and culture of squamous cell carcinoma lines. Methods Mol Biol 2011;731:151–9.
12. Chapman CM, Sun X, Roschewski M, Aue G, Farooqui M, Stennett L, et al. ON 01910.Na is selectively cytotoxic for chronic lymphocytic leukemia cells through a dual mechanism of action involving PI3K/AKT inhibition and induction of oxidative stress. Clin Cancer Res 2012;18:1979–91.
13. Prasad A, Khudaynazar N, Tantravahi RV, Gillum AM, Hoffman BS. ON 01910.Na (rigosertib) inhibits PI3K/Akt pathway and activates oxidative stress signals in head and neck cancer cell lines. Oncotarget 2016;7:79388–400.
14. Prasad A, Park IW, Allen H, Zhang X, Reddy MV, Boominathan R, et al. Styryl sulfonyl compounds inhibit translation of cyclin D1 in mantle cell lymphoma cells. Oncogene 2009;28:1518–28.
15. Athuluri-Divakar SK, Vasquez-Del Carpio R, Dutta K, Baker SJ, Cosenza SC, Basu I, et al. A small molecule RAS-mimetic disrupts RAS association with effector proteins to block signaling. Cell 2016;165:643–55.
16. Jost M, Chen Y, Gilbert LA, Horlbeck MA, Krenning L, Menchon G, et al. Combined CRISPRi/a-based chemical genetic screens reveal that rigosertib is a microtubule-destabilizing agent. Mol Cell 2017;68:210–223.
17. Hugle M, Belz K, Fulda S. Identification of synthetic lethality of PLK1 inhibition and microtubule-destabilizing drugs. Cell Death Differ 2015;22:1946–56.
18. Silverman LR, Greenberg P, Raza A, Olnes MJ, Holland JF, Reddy P, et al. Clinical activity and safety of the dual pathway inhibitor rigosertib for higher risk myelodysplastic syndromes following DNA methyltransferase inhibitor therapy. Hematol Oncol 2015;33:57–66.
19. Anderson RT, Keysar SB, Bowles DW, Glogowska MJ, Astling DP, Morton JJ, et al. The dual pathway inhibitor rigosertib is effective in direct patient tumor xenografts of head and neck squamous cell carcinomas. Mol Cancer Ther 2013;12:1994–2005.
20. Konieczkowski DJ, Johannessen CM, Garraway LA. A convergence-based framework for cancer drug resistance. Cancer Cell 2018;33:801–15.